JACS
JOURNAL OF THE AMERICAN CHEMICAL SOCIETY

ARTICLE

pubs.acs.org/JACS

Effect of Molecular Packing on Corannulene-Based Materials Electroluminescence

Laura Zoppi,[†] Layla Martin-Samos,[‡] and Kim K. Baldridge*[,†]

[†]University of Zürich, Winterthurerstrasse 190, CH-8057 Zürich, Switzerland

[‡]CNR-IOM DEMOCRITOS, via Bonomea 265, 34136 Trieste, Italy

Supporting Information

ABSTRACT: The present investigation reports for the first time a detailed theoretical analysis of the optical absorption spectra of corannulene-based materials using state-of-the-art first-principles many-body GW-BSE theory. The study specifically addresses the nature of optical excitations for predictions regarding suitability for device fabrication. The well-defined structure−correlation relationship in functionalized corannulenes is used in a focused investigation of the predicted optoelectronic properties in both the isolated state and bulk crystals. The findings suggest that the excitonic properties are strongly dependent on the specific substituent group as well as the crystalline arrangement. Arylethynyl-substituted corannulene derivatives are shown to be the most suitable for device purposes.

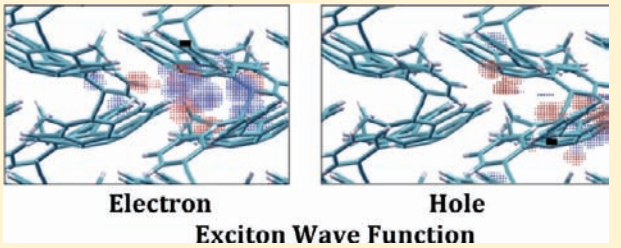

The strong potential for new technological applications incorporating organic semiconductors and conducting π-conjugated aromatic molecules has emerged as one of the hottest research areas in both academia and industry and holds promise for the development of large-scale, low-cost, flexible electronic devices.[1] To utilize new organic materials successfully in technologies such as organic light-emitting diodes (OLEDs),[2−5] organic photovoltaic cells (OPVCs),[6−9] and organic field-effect transistors (OFETs),[10−13] it is of fundamental importance to address the specific nature of the electrical/photogenerated states.

Significant breakthroughs have resulted from the design of specifically tuned molecules from first principles. In this work, the focus is on a specially designed set of molecules based on the smallest nonplanar fullerene fragment, corannulene ($C_{20}H_{10}$).[14] The relative ease of preparation of this fivefold-symmetric molecule and the ability to tailor specialized properties,[15] including access to chiral derivatives,[16] enables the exploration of a wealth of phenomenology not only for single molecules[17−20] but also for molecules deposited on metal surfaces[21] or packed in crystalline environments.[22,23] Importantly, it has been well-demonstrated that functionalization of the bowl periphery is directly correlated with predictable dynamic behavior, with several derivatives having tunable optoelectronic properties.[23−25] In particular, arylethynyl derivatives display high fluorescence quantum yields (0.8−0.9)[23] and tunable emission wavelengths depending on the number and exact nature of the functional group, and they yield columnar arrangements in the crystalline environment.[23] In contrast, the parent compound, corannulene, is only a modest fluorophore and packs in the crystal phase without columnar order. This set of photophysically tunable organic active materials requires in-depth investigation of the mechanism associated with their optoelectronic properties in order to predict their potential applicability in device applications.

Limitations in experiment as well as theory have made progress in this field slow. Typical experiments are carried out in solution, where the influence of solvent, dynamics, and disorder effects, make interpretation of the spectra quite difficult. Moreover, despite the weak nature of the interactions in crystalline organic solids, packing effects have been shown to have a strong influence on the nature of the optical transitions.[26−29] Computationally affordable theoretical methods for accurate predictions are also very few, particularly for π-conjugated molecular systems. Application of standard many-body theories, which are widely used in solid-state physics, is far from obvious for these systems.[30−32] Time-dependent density functional theory (TD-DFT) offers a good compromise between accuracy and computational cost,[33,34] although the errors can be significant for large organic chromophores and are highly dependent on the functional parametrization used. The situation becomes even more complicated when considering crystals of organic molecules, where the complexity and size of the systems represent a real challenge for theoretical investigations.[35−37]

The present investigation reports for the first time a detailed theoretical analysis of optical absorption spectra describing excitonic effects in corannulene-based materials that specifically addresses the nature of optical excitations for predictions regarding suitability for device fabrication. The intriguing electronic properties of the parent, corannulene, can be ascribed to its large intrinsic dipole moment (2.01 D)[38] and its shallow bowl depth (8.7 nm), which imparts dynamic properties characterized by a

Received: May 3, 2011
Published: July 28, 2011

Scheme 1. Structures of Corannulene (1), 1,6-Dimethylcorannulene (2), 1,2,5,6-Tetramethylcorannulene (3), 1,6-Diphenylethynylcorannulene (4), and 1,2,5,6-Tetraphenylethynylcorannulene (5)

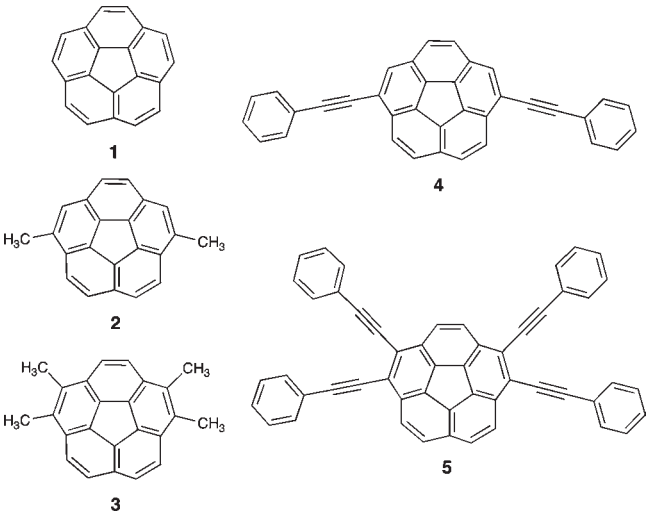

Table 1. First Singlet Excitons (S), First Triplet Excitons (T), and GW HOMO−LUMO Gaps (All Values in eV) for the Series 1−5 Depicted in Scheme 1

molecule	S	T	Δ(S/T)[b]	GW HOMO−LUMO gap
1	3.60 (3.64)[a]	2.67 (2.72)[a]	0.93 (0.92)	7.16
2	3.46	2.56	0.90	7.06
3	3.33	2.55	0.78	7.53
4	3.08 (3.07)[a]	1.93	1.15	5.41
5	2.87 (2.92)[a]	1.74	1.13	5.57

[a] The value in parentheses is the corrected experimental value for the 0−0 absorption band obtained using the perturbation method of Grimme et al,[34] which employs the appropriate system-specific corrections for solvent environment, geometric reorganization, and vibrational effects for the system of interest and the level of theory: $\Delta E^{\mathrm{vert,exptl(vacuum)}} = \Delta E^{(0-0),\mathrm{exptl(solv)}} + \Delta E^{\mathrm{relax}} + \Delta E^{\mathrm{solv}}$. [b] ΔE(first singlet exciton − first triplet exciton), in eV.

bowl-to-bowl inversion barrier of 11.5 kcal/mol.[18] Experimental and computational investigations of a large series of substituted derivatives have nicely established a predictable correlation between the structure (bowl depth) and the barrier to bowl inversion.[18] For the present purpose, two classes of substituent types were chosen to demonstrate the variation in properties for the following alkyl derivatives and arylethynyl derivatives: corannulene (**1**), 1,6-dimethylcorannulene (**2**), 1,2,5,6-tetramethylcorannulene (**3**), 1,6-diphenylethynylcorannulene (**4**), and 1,2,5,6-tetraphenylethynylcorannulene (**5**) (Scheme 1). Alkyl rim substituents have been observed to decrease the bowl depth and thus the inversion barrier relative to that of **1**. For example, **2** has a bowl depth of 6.6 nm and an interconversion barrier of 9.0 kcal/mol.[18,23] In contrast, arylethynyl substituents increase the bowl depth and give a higher barrier, as a function of the number of arylethynyl groups.[23] In the present work, we have predicted the influence on the optical absorption spectra of substituent-related fine-tuning of the bowl depth (by some

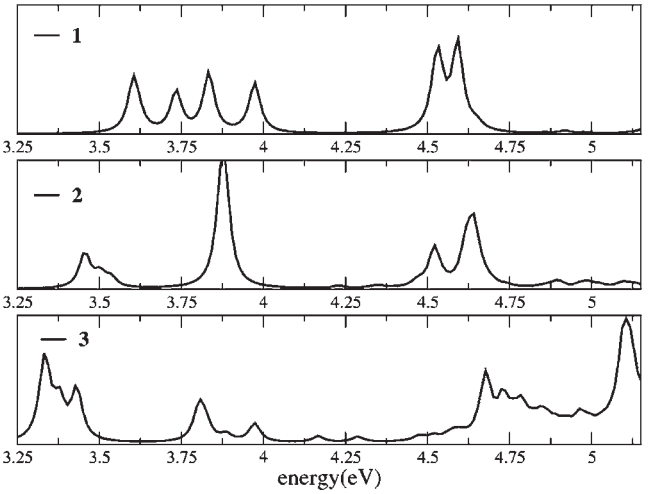

Figure 1. GW-BSE-predicted optical absorption spectra (in arbitrary units) for corannulene (**1**), 1,6-dimethylcorannulene (**2**), and 1,2,5,6-tetramethylcorannulene (**3**). An artificial Lorentzian broadening of 0.02 eV was used.

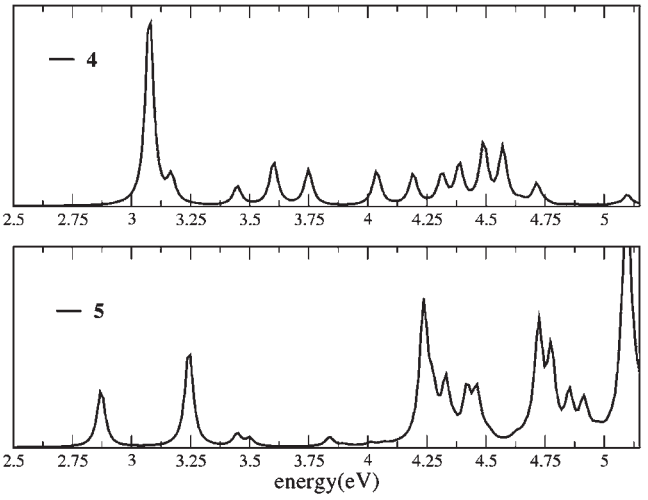

Figure 2. GW-BSE-predicted optical absorption spectra (in arbitrary units) for 1,6-diphenylethynylcorannulene (**4**) and 1,2,5,6-diphenylethynlcorannulene (**5**). An artificial Lorentzian broadening of 0.02 eV was used.

tenths of a nanometer) and of various packing motifs, by considering the systems in both the isolated state and the bulk crystal. The calculations were carried out using the first-principles many-body GW-BSE (Bethe−Salpeter) approach,[39,40] which is considered a state-of-the-art methodology for the study of electronic excitations of materials.[40−44] The results are compared to experimental solution-phase emission and fluorescence data[23,45] and X-ray crystal data.[23]

Reliable and predictive treatments of the excitonic nature of optical excitation are quite sensitive, and currently there is an open debate about the nature of such treatments,[31] including the challenges associated with valid comparisons with experimental data. Table 1 shows the onset of optical absorption for systems **1**−**5** predicted in this work using GW-BSE calculations together with experimental data (where available) for comparison. The predictions are within 0.1 eV of the experimental values, where

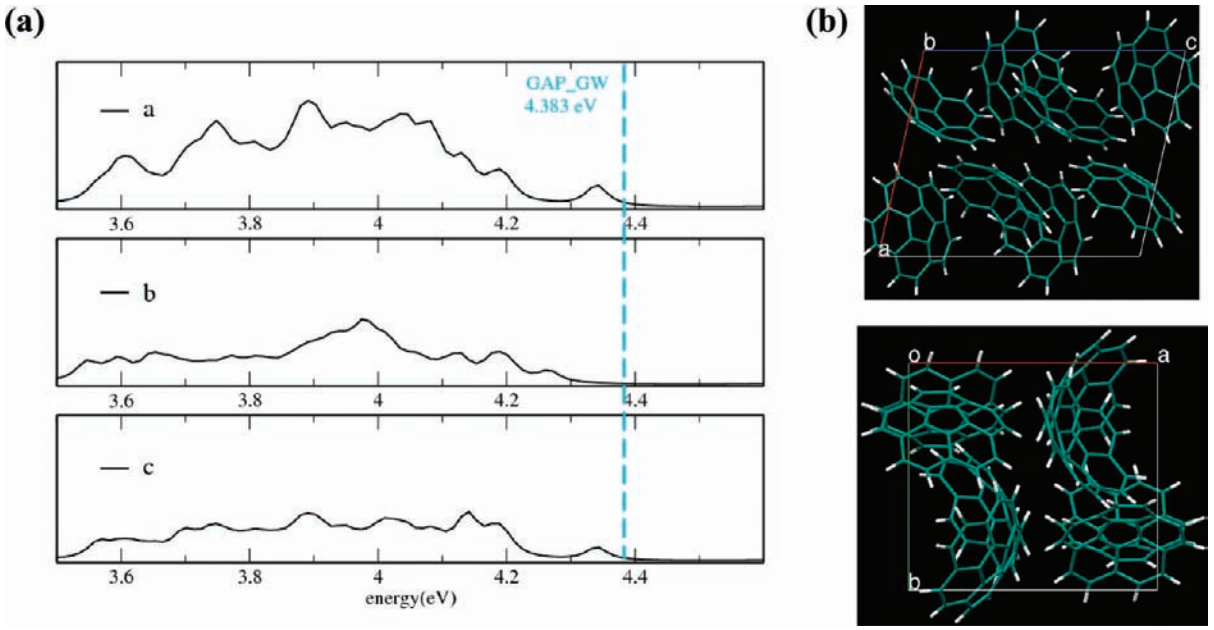

Figure 3. (a) GW-BSE-predicted optical absorption spectra (in arbitrary units) of crystalline corannulene (**1**) along the three crystallographic directions (an artificial Lorentzian broadening of 0.02 eV was used). (b) Views of the crystal structure of **1**.

the latter have been corrected using a recently demonstrated strategy to account for experimental conditions pertinent to the level of theory being used.[34]

Electrical injection of charges in the organic active element of a device can lead to the generation of triplet and singlet excitations, which typically display different relaxed geometries. Because of the possibility of exchange between like spins, triplet wave functions typically display a more spatially confined character, a feature that is particularly pronounced for low-lying excitations with a corresponding higher binding energy. Knowledge of the singlet−triplet energy difference enables fine-tuning to minimize triplet-gain quenching as well as general improvements in device performance, as was recently shown for triphenylene-based polymers.[46] In the present molecular systems, the energy separation between the first singlet and first triplet (i.e., the exchange energy[47]) remains essentially constant in the range 0.8−1.2 eV (Table 1), which is within the bounds for conjugated polymers.[46]

The calculated optical absorption spectra for the full set of corannulene derivatives in their isolated states predict a general red shift with increasing number and size of the substituents (Figures 1 and 2). Further analysis of the molecular states of **4** and **5** shows that the most bound exciton is dominated by a HOMO → LUMO transition at ∼3 eV (3.1 and 2.9 eV, respectively). In the former case, this exciton is also the primary absorption peak. On the other hand, the methyl-substituted systems are dominated by a HOMO → LUMO+1 transition at ∼3.5 eV (3.5 and 3.3 eV, respectively). The parent corannulene has no clear dominant transition of the most bound exciton. This difference between the first exciton compositions for the two classes of substituted systems reflects the difference in degeneracy of their corresponding frontier orbitals. Interestingly, in the parent corannulene, the second exciton is a dark exciton that is nearly degenenerate with the first exciton and could be an important nonradiative channel explaining a source of fluorescence quenching.

Prediction of the potential applicability of organic materials in devices requires consideration of their optical properties with regard to the crystalline structure. The specific X-ray crystal structural details for **1**−**5** can be found in our previously published work.[23] The parent **1** crystallizes in the monoclinic space group (Figure 3b) without showing any particular columnar order. In contrast, the functionalized derivatives tend to pack in either an orthorhombic or a monoclinic unit cell and show a columnar arrangement along one particular stacking axis (Figures 4b, 5b, 6b, and 7b).

The traditional picture of the energetic excitonic structure of an organic crystal[48] (Figure 8) shows for both the singlet and triplet states the weakly bound charge transfer (CT) excitons (S_{CT} and T_{CT}), which are characterized by different spatial locations of the electron and the hole, and the more strongly bound direct excitons (S_D and T_D), where the electron and hole instead occupy the same spatial region. Theoretical predictions of the first singlet excitons, first triplet excitons, and the energy band gaps for crystalline **1**−**5** are reported in Table 2. Within the same class of functional group, one sees a moderate decrease in excitation energy with increasing number and size of substituent. Over all of the crystals, there is an average first singlet/first triplet splitting, Δ(S/T), of 0.5 eV (Table 2), with a notably larger value (0.6 eV) for **2**. Thus, in going from the isolated molecules to the bulk crystal, an effect of packing appears to be a general decrease in exchange energy of ∼0.5 eV [compare the Δ(S/T) values in Tables 1 and 2]. The GW-predicted energy band gaps also decrease by over 2 eV in going from the isolated molecules to the crystals. The data show a fairly consistent band gap (avg 4.3 eV) for corannulene and the dimethyl derivatives (Table 2), while that for the arylethynyl derivatives is ∼1 eV smaller (avg 3.4 eV).

A sizable contribution of the spectrum at the free electron−hole threshold (GW gap) is an indication of the existence of light-coupled states available for the recombination of injected electrons and holes that can afterward emit light (OLEDs).[49] In particular, CT states lying energetically near the electron−hole

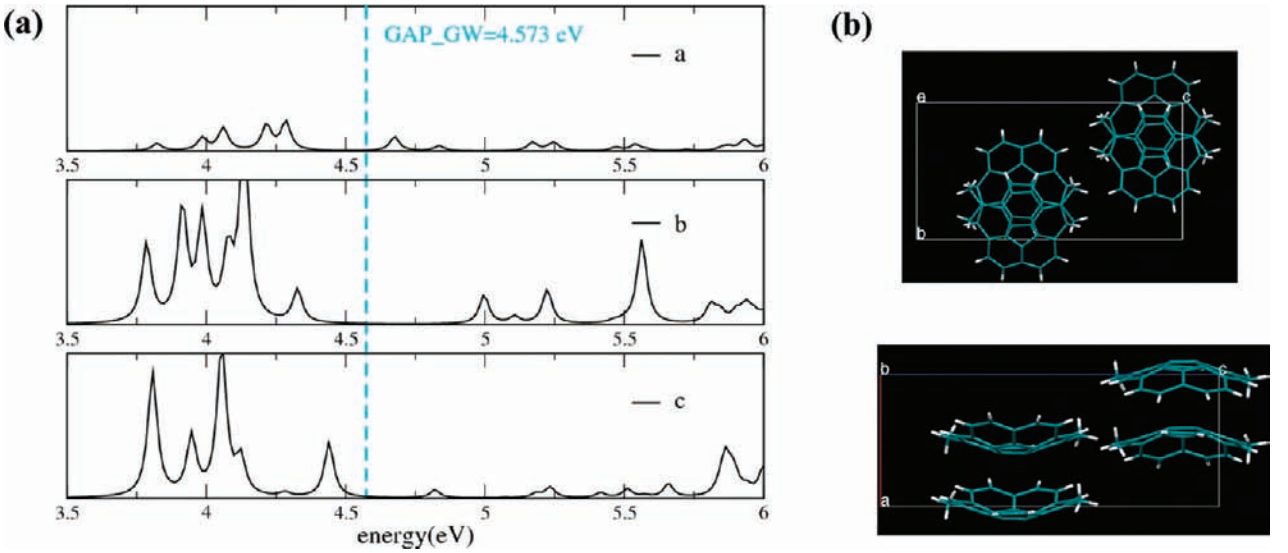

Figure 4. (a) GW-BSE-predicted optical absorption spectra (in arbitrary units) of crystalline 1,6-dimethylcorannulene (**2**) along the three crystallographic directions (an artificial Lorentzian broadening of 0.02 eV was used). (b) Views of the crystal structure of **2**.

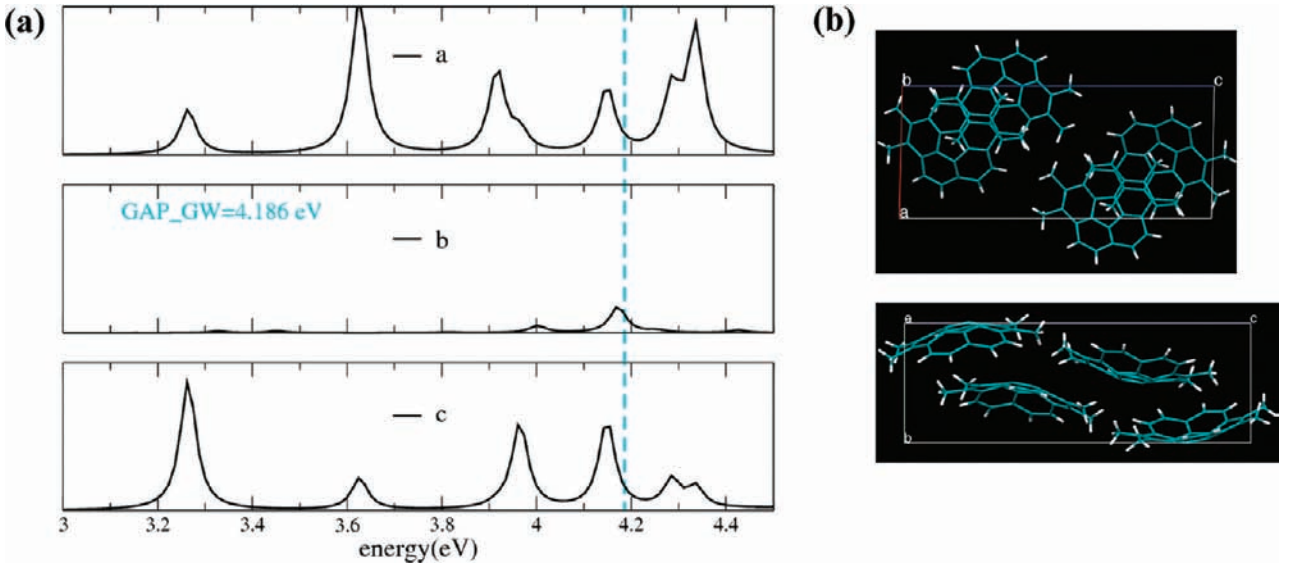

Figure 5. (a) GW-BSE-predicted optical absorption spectra (in arbitrary units) of crystalline 1,2,5,6-tetramethylcorannulene (**3**) along the three crystallographic directions (an artificial Lorentzian broadening of 0.02 eV was used). (b) Views of the crystal structure of **3**.

continuum (Figure 8) are the most effective for typical device purposes. In order to investigate this further for the set of systems under consideration, the optical absorption spectra were calculated along each of the three crystallographic directions, as illustrated in panels (a) of Figures 3−7. For **1**−**3**, the spectra are almost featureless in this energy region, independent of the crystallographic direction considered. For **1**, the spectrum does not show any contribution close to the free electron−hole threshold. Derivatives **2** and **3** show very small contributions close to the energy gap (4.33 and 4.15 eV, respectively). Thus, the methyl-substituted materials would not be considered promising for electroluminescence device purposes because their electronic states close to the energy gap are coupled poorly with light.

The picture significantly changes when crystals of phenylethynyl derivatives **4** and **5** are considered. In their respective optical absorption spectra (Figures 6a and 7a), these two crystals display important contributions along one or more of the three crystallographic directions just in the region of the GW gap. In **4**, a major contribution is detected along the *b* direction (Figure 6a), coinciding with the direction of the long arms of the substituent groups (Figure 6b). There is also some contribution along the *a* direction but no contribution along the stacking direction. In **5**, the direction of the maximum contribution shown in Figure 7a again corresponds with that of the long arms of the substituents (Figure 7b), while the spectrum appears featureless in the other two directions. The lack of light absorption along the direction of the stacks is consistent with the strong anisotropy of the π-conjugated systems and the wide intermolecular space in this direction.

In the particular case of OLEDs, in order to achieve efficient luminescence, it is necessary to have a good balance of the electron

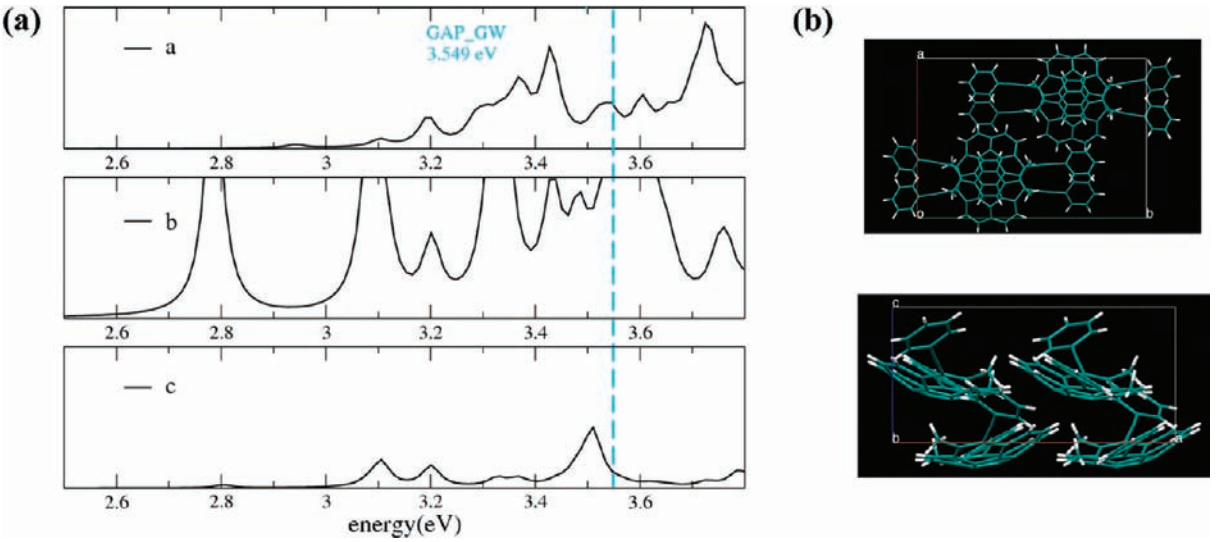

Figure 6. (a) GW-BSE-predicted optical absorption spectra (in arbitrary units) of crystalline 1,6-diphenylethynylcorannulene (**4**) along the three crystallographic directions (an artificial Lorentzian broadening of 0.02 eV was used). (b) Views of the crystal structure of **4**.

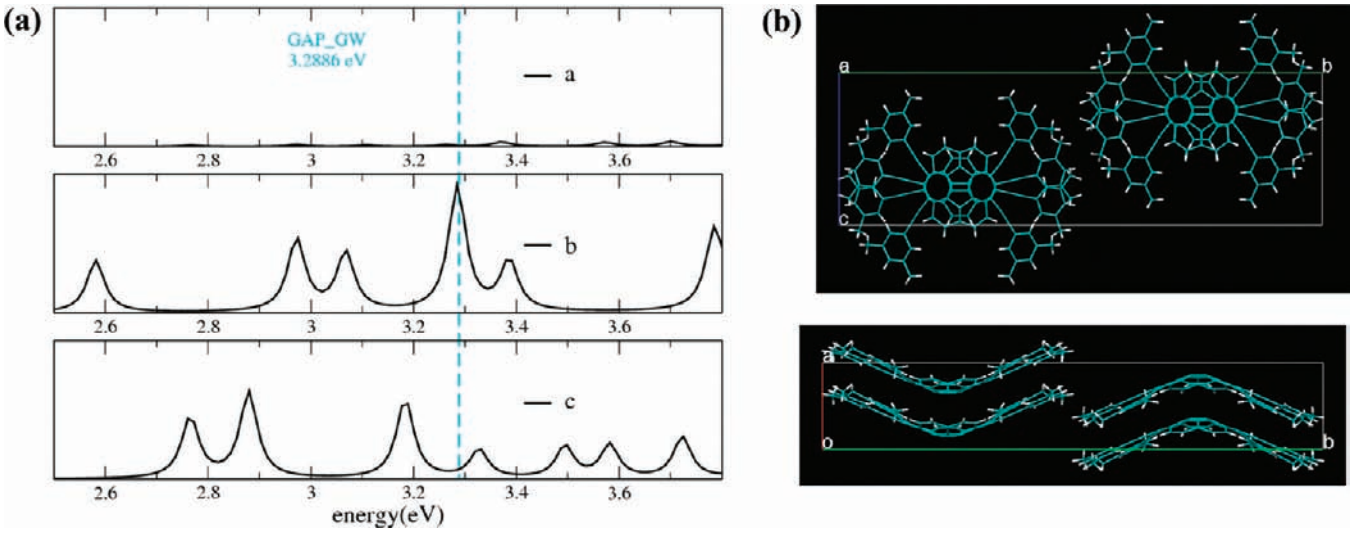

Figure 7. (a) GW-BSE-predicted optical absorption spectra (in arbitrary units) of crystalline 1,2,5,6-tetraphenylethynylcorannulene (**5**) along the three crystallographic directions (an artificial Lorentzian broadening of 0.02 eV was used). (b) Views of the crystal structure of **5**.

and hole currents with efficient capture of electrons and holes in excitonic states within the emissive layer.[49] Because electrons and holes are injected into the materials at random positions, it is much more effective for the excitons to be as delocalized as possible (CT excitons) in order to maximize the probability of capture of the random charge carriers. The specific nature of the excitons in an organic material has been shown to depend strongly on the symmetry and packing motif displayed in the crystalline phase.[26] It is therefore of great interest in the present work to investigate the solid-state effects on the specific nature (direct or CT) of the excitons in the crystals by looking at the shapes of the exciton wave functions in the different crystalline arrangements. To carry this out, the exciton wave functions were evaluated (a) by fixing the hole at the position that maximizes the electron probability and (b) by fixing the electron at the position that maximizes the hole probability. It should be noted that the precision in the estimation of the electron and hole positions is on the order of 1 Å. This evaluation enabled the crystalline packing motifs to be correlated with the corresponding nature of the excitons in the bulk and ultimately clarified and predicted the optoelectronic behavior of the different materials.

In the parent compound **1**, the exciton wave function for the first bright exciton (3.62 eV) shows that the electron and hole can be found at different spatial locations in the crystal; the electron is delocalized over different corannulene units on the concave and convex parts of the bowl, whereas the hole is mostly concentrated within the intramolecular space. The electron−hole wave function in this case does not show a particular pattern, reflecting also the crystalline packing arrangement, which has different orientations of the molecules within the unit cell.

The exciton wave function for **2**, corresponding to an energy of 4.33 eV, which is just below the energy gap, is shown in Figure 9 (a,b). The shape of the wave function shows that the electron (Figure 9a) is delocalized partly on the upward pointing

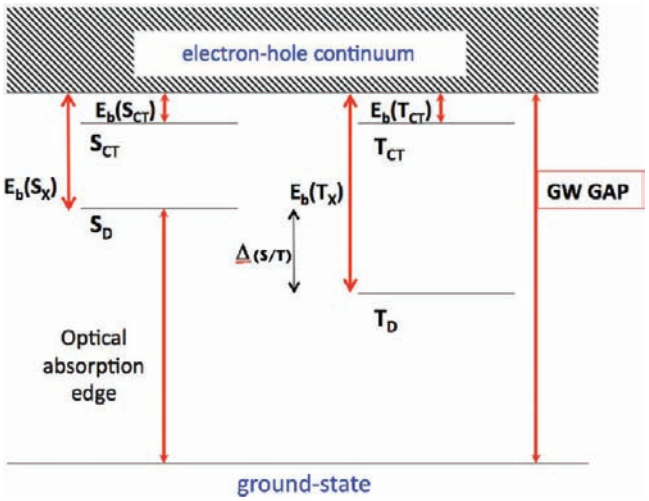

Figure 8. Energy level diagram showing the singlet and triplet charge transfer (CT) excitons (S_{CT} and T_{CT}, respectively) and the lowest direct (D) singlet and triplet excitons (denoted by S_D and T_D, respectively). The exchange energy $\Delta(S/T)$ (i.e., $S_D - T_D$) is also shown.

Table 2. GW-BSE-Calculated First Singlet Excitons (S), First Triplet Excitons (T), and GW Energy Band Gaps (All Values in eV) for Corannulene (1) and the Four Functionalized Derivatives 2−5

crystal	S	T	$\Delta(S/T)^a$	GW energy band gap
1	3.32	2.85	0.47	4.38
2	3.79	3.14	0.64	4.57
3	3.26	2.82	0.44	4.19
4	2.79	2.30	0.49	3.55
5	2.58	2.12	0.46	3.29

[a] ΔE(first singlet exciton − first triplet exciton), in eV.

bowl and partly within the interchain space; the hole (Figure 9b) is delocalized partly on the downward-pointing bowl and partly within the interchain space. There is a significant amount of CT between adjacent molecules along the *b* direction and, to a minor extent, between molecules belonging to different stacks. The CT between adjacent molecules is mediated by the methyl groups and bowl-to-bowl $\pi-\pi$ interactions. The poor coupling of these states with light (e.g., the optical absorption spectrum) makes this material not a practical choice for device purposes.

Figure 9 (c,d) shows the exciton wave function for the electron and the hole for **3**, corresponding to an energy of 4.15 eV, which is just below the fundamental gap. The tilting of the molecules with respect to the stacking axis (Figure 5b) results in electron and hole delocalization on the same submolecular units, partly on the central molecular bowls and partly within the interchain space along the *b* direction. The delocalization is therefore more effective between adjacent molecules belonging to different columns rather than in the direction of the molecular stacking. The direct nature of the exciton together with the poor coupling with light (e.g., the optical absorption spectrum) impedes the use of this material in electronic devices.

According to this analysis, neither methyl-substituted corannulene materials shows potential for use as an active species for optoelectronics, not only because of the optical absorption spectrum profile but also because of the specific nature of the excitons in the bulk. The CT character is mostly mediated by the presence of the methyl substituent. This enables molecular subunits to approach quite close to each other, facilitating bowl-to-bowl interactions in a direction perpendicular to the stack.

The picture changes significantly with the phenylethynyl derivatives, where the long arms of the substituents isolate the cores of the bowls much more effectively. This difference in packing motif leads to completely different exciton arrangements. The exciton wave function of **4** that is closest in energy to the GW gap (3.54 eV) is shown in Figure 10 (a,b). The electron is localized mainly within the intramolecular space between two of the four molecular units in the unit cell and to a very minor extent on the other two subunits (Figure 10a). The hole is concentrated directly on the molecule cores rather than within the free space between them (Figure 10b). The electron distribution suggests a "hopping" mechanism between two molecular units along the stacking direction. This spatial distribution is more likely to occur within a crystalline environment, where the intermolecular space along the stack is wide enough to enable a proper accommodation of the electron distribution. Thus, the CT process can occur between molecules of the same column along the stacking direction but not between molecules of adjacent stacks. The strong coupling with light (e.g., the optical absorption spectrum) and the CT nature of the exciton are extremely promising for OLED performance.

The exciton wave function of **5** that is closest in energy to the GW gap (3.28 eV) is depicted in Figure 10 (c,d). The underlying crystalline structure, which is characterized by opposing orientations of the bowl concavity in adjacent stacks (Figure 7b), causes a different spatial organization for the exciton in comparison with **4**. The electron and hole are localized on the same two submolecular units, with a preference for two molecules pointing in the same direction, but in contrast to **4**, they are not spatially separated, giving rise to a well-defined direct exciton. The primary localization in either case is on the extremity of the external substituents and in the intermolecular space along the stacking direction rather than on the central corannulene core. Despite the existence of such a state close to the fundamental gap, the material is still promising for light-emitting purposes, although less so than **4** because of the localized nature of the exciton.

The most striking advance in this investigation is the ability to predict the molecular substitution/packing motifs most suitable for device purposes. A key factor is the possibility of tuning the optoelectronic properties by modifying the structure (bowl depth) on the nanoscale in a controllable way. The arylethynyl substituents lead to a smaller GW gap in both the isolated state and the crystalline environment. Moreover, the excitonic electronic properties in the bulk systems depend not only on the specifics of the packing (noncolumnar vs columnar, variations in columnar motifs) but also on the specific nature of the substituent attached to the parent compound. For small substituents (e.g., methyl groups), the possibility for the molecules to approach close to each other leads to CT or direct excitons in a columnar packing structure, with alternating bowl directionality between adjacent stacks, depending on the molecular orientation. The larger phenylethynyl substituents enable better isolation of the central cores of adjacent bowls, leading to a well-defined CT or direct exciton, according to the mutual orientation of the bowl openings in adjacent columns.

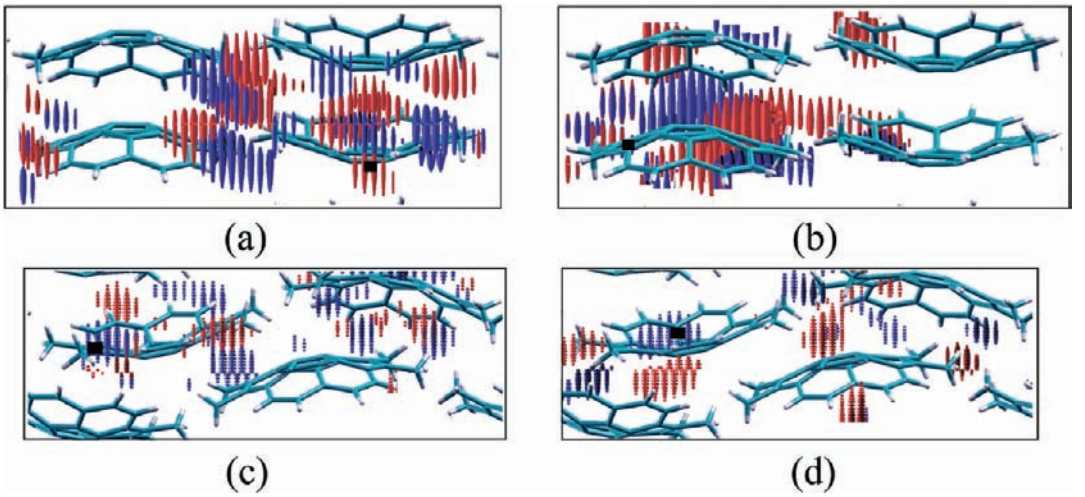

Figure 9. (a, b) Exciton wave function corresponding to an energy of 4.33 eV in the crystalline form of 1,6-dimethylcorannulene (**2**) for (a) the electron (the hole position is indicated by the black rectangle) and (b) the hole (the electron position is indicated by the black rectangle). (c, d) Exciton wave function corresponding to an energy of 4.15 eV in the crystalline form of 1,2,5,6-tetramethylcorannulene (**3**) (*bc* plane) for (c) the electron (the hole position is indicated by the black rectangle) and (d) the hole (the electron position is indicated by the black rectangle).

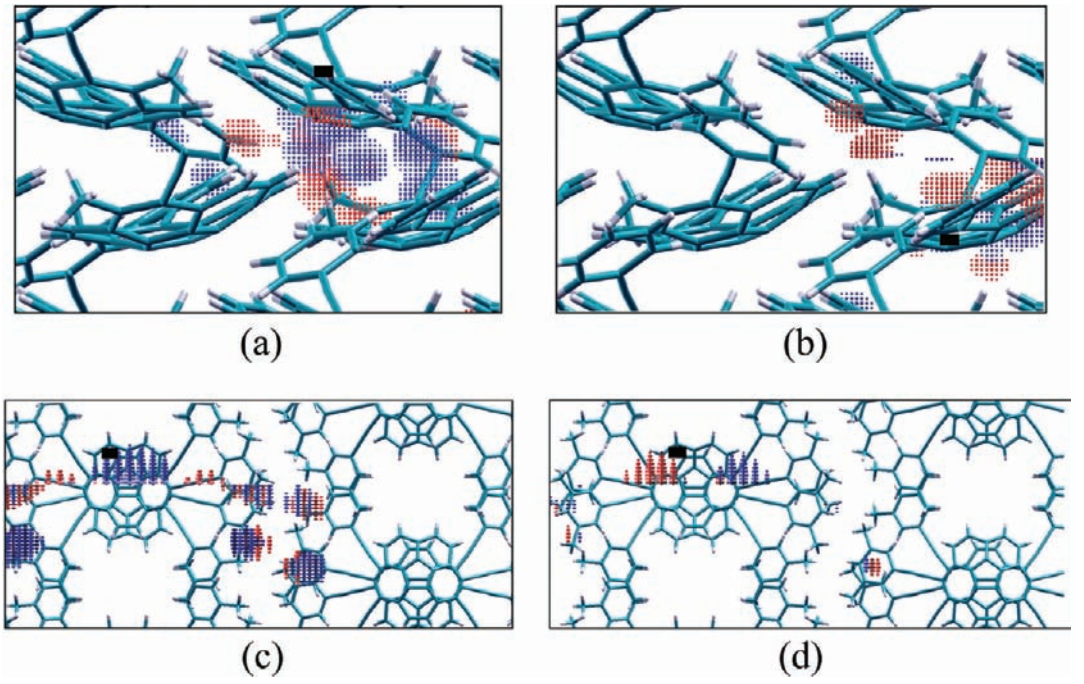

Figure 10. (a, b) Exciton wave function corresponding to an energy of 3.54 eV in the crystalline form of 1,6-diphenylethynylcorannulene (**4**) (*ac* plane) for (a) the electron (the hole position is indicated by the black rectangle) and (b) the hole (the electron position is indicated by the black rectangle. (c, d) Exciton wave function corresponding to an energy of 3.28 eV in the crystalline form of 1,2,5,6-tetraphenylethynylcorannulene (**5**) (*bc* plane) for (c) the electron (the hole position is indicated by the black rectangle) and (d) the hole (the electron position is indicated by the black rectangle).

For OLED targets, arylethynyl substitution provides a material with a smaller fundamental gap and a sizable number of states close to fundamental gap that are strongly coupled with light and available for charge recombination. Moreover, columnar crystal packing in which all of the molecules within the stacks face the same direction, is most suitable for generating charge transfer and most effective for charge recombination. Future studies will investigate additional substituent groups that show promise for optimal properties of this type, such as indenocorannulenes[50] and (phenylthio)$_n$corannulenes.

■ ASSOCIATED CONTENT

Supporting Information. Additional computational details concerning the GW calculations, additional data concerning the importance of including local fields in the calculations, as well

as crystal structures, computationally optimized structures and energetics. This material is available free of charge via the Internet at http://pubs.acs.org.

AUTHOR INFORMATION

Corresponding Author
kimb@oci.uzh.ch

ACKNOWLEDGMENT

This work was supported by the Swiss National Science Foundation. We thank the Swiss National Supercomputing Center for a grant of computer time. Dr. Alice Ruini, Dr. Giovanni Bussi, and Prof. Dr. Jay Siegel are acknowledged for useful discussions.

REFERENCES

(1) Forrest, S. R. *Nature* **2004**, *428*, 911.
(2) Chen, W.; Qi, D.-C.; Huang, H.; Gao, X.; Wee, A. T. S. *Adv. Funct. Mater.* **2011**, *21*, 410.
(3) Müller, C. D.; Falcou, A.; Reckefuss, N.; Rojahn, M.; Wiederhirn, V.; Rudati, P.; Frohne, H.; Nuyken, O.; Becker, H.; Meerholz, K. *Nature* **2003**, *421*, 829.
(4) Baldo, M. A.; Thompson, M. E.; Forrest, S. R. *Nature* **2000**, *403*, 750.
(5) Reineke, S.; Linder, F.; Schwartz, G.; Seidler, N.; Walzer, K.; Lüssem, B.; Leo, K. *Nature* **2009**, *459*, 234.
(6) Hagfeldt, A.; Grätzel, M. *Acc. Chem. Res.* **2000**, *33*, 269.
(7) Peumans, P.; Yakimov, A.; Forrest, S. R. *J. Appl. Phys.* **2003**, *93*, 3693.
(8) O'Regan, B.; Grätzel, M. *Nature* **1991**, *353*, 737.
(9) Dennler, G.; Scharber, M. C.; Brabec, C. J. *Adv. Mater.* **2009**, *21*, 1323.
(10) Katz, H. E.; Lovinger, A. J.; Johnson, J.; Kloc, C.; Siegrist, T.; Li, W.; Lin, Y. Y.; Dodabalapur, A. *Nature* **2000**, *404*, 478.
(11) Crone, B.; Dodabalapur, A.; Lin, Y.-Y.; Filas, R. W.; Bao, Z.; LaDuca, A.; Sarpeshkar, R.; Katz, H. E.; Li, W. *Nature* **2000**, *403*, 521.
(12) Chua, L.-L.; Zaumseil, J.; Chang, J.-F.; Ou, E. C. W.; Ho, P. K. H.; Sirringhaus, H.; Friend, R. H. *Nature* **2005**, *434*, 194.
(13) Jurchescu, O. D.; Popinciuc, M.; Wees, B. J. v.; Palstra, T. T. M. *Adv. Mater.* **2007**, *19*, 688.
(14) Seiders, T. J.; Baldridge, K. K.; Siegel, J. S. *J. Am. Chem. Soc.* **1996**, *118*, 2754.
(15) Wu, Y.-T.; Siegel, J. S. *Chem. Rev.* **2006**, *106*, 4843.
(16) Fasel, R.; Parschau, M.; Ernst, K.-H. *Angew. Chem., Int. Ed.* **2003**, *42*, 5178.
(17) Borchardt, A.; Fuchicello, A.; Kilway, K. V.; Baldridge, K. K.; Siegel, J. S. *J. Am. Chem. Soc.* **1992**, *114*, 1921.
(18) Seiders, T. J.; Baldridge, K. K.; Grube, G. H.; Siegel, J. S. *J. Am. Chem. Soc.* **2001**, *123*, 517.
(19) Seiders, T. J.; Baldridge, K. K.; Gleiter, R.; Siegel, J. S. *Tetrahedron Lett.* **2000**, *41*, 4519.
(20) Baldridge, K. K.; Siegel, J. S. *Theor. Chem. Acc.* **1997**, *97*, 67.
(21) Parschau, M.; Fasel, R.; Ernst, K.-H.; Grönig, O.; Brandenberger, L.; Schillinger, L.; Greber, T.; Seitsonen, A. P.; Wu, Y.-T.; Siegel, J. S. *Angew. Chem., Int. Ed.* **2007**, *46*, 8258.
(22) Filatov, A. S.; Scott, L. T.; Petrukhina, M. A. *Cryst. Growth Des.* **2010**, *10*, 4607.
(23) Wu, Y. T.; Bandera, D.; Maag, R.; Linden, A.; Baldridge, K. K.; Siegel, J. S. *J. Am. Chem. Soc.* **2008**, *130*, 10729.
(24) Mack, J.; Vogel, P.; Jones, D.; Kaval, N.; Sutton, A. *Org. Biomol. Chem* **2007**, *5*, 2448.
(25) Valenti, G.; Bruno, C.; Rapino, S.; Fiorani, A.; Jackson, E. A.; Scott, L. T.; Paolucci, F.; Marcaccio, M. *J. Phys. Chem. C* **2010**, *114*, 19467.
(26) Ruini, A.; Caldas, M. J.; Bussi, G.; Molinari, E. *Phys. Rev. Lett.* **2002**, *88*, 206403.
(27) Bussi, G.; Ruini, A.; Molinari, E.; Caldas, M. J.; Puschnig, P.; Ambrosch-Draxl, C. *Appl. Phys. Lett.* **2002**, *80*, 4118.
(28) Ferretti, A.; Ruini, A.; Molinari, E.; Caldas, M. J. *Phys. Rev. Lett.* **2003**, *90*, 086401.
(29) Bussi, G.; Ferretti, A.; Ruini, A.; Caldas, M. J.; Molinari, E. *Adv. Solid State Phys.* **2003**, *43*, 313.
(30) Palumno, M.; Hogan, C.; Sottile, F.; Bagalá, P.; Rubio, A. *J. Chem. Phys.* **2009**, *131*, 084102.
(31) Rocca, D.; Lu, D.; Galli, G. *J. Chem. Phys.* **2010**, *133*, 164109.
(32) Kaasbjerg, K.; Thygesen, K. S. *Phys. Rev. B* **2010**, *81*, 085102.
(33) Dierksen, M.; Grimme, S. *J. Phys. Chem. A* **2004**, *108*, 10225.
(34) Goerigk, L.; Moellmann, J.; Grimme, S. *Phys. Chem. Chem. Phys.* **2009**, *11*, 4611.
(35) Tiago, M. L.; Northrup, J. E.; Louie, S. G. *Phys. Rev. B* **2003**, *67*, 115212.
(36) Sai, N.; Tiago, M. L.; Chelikowsky, J. R.; Reboredo, F. A. *Phys. Rev. B* **2008**, *77*, 161306(R).
(37) Ambrosch-Draxl, C.; Nabok, D.; Puschnig, P.; Mesenbichler, C. *New J. Phys.* **2009**, *11*, 125010.
(38) Lovas, F. J.; McMahon, R. J.; Grabow, J.-U.; Schnell, M.; Mack, J.; Scott, L. T.; Kuczkowski, R. L. *J. Am. Chem. Soc.* **2005**, *127*, 4345.
(39) Hedin, L. *Phys. Rev.* **1965**, *139*, A796.
(40) Onida, G.; Reining, L.; Rubio, A. *Rev. Mod. Phys.* **2002**, *74*, 601.
(41) Rohlfing, M.; Louie, S. G. *Phys. Rev. Lett.* **1998**, *81*, 2312.
(42) Rohlfing, M.; Louie, S. G. *Phys. Rev. Lett.* **1999**, *82*, 1959.
(43) Rohlfing, M.; Louie, S. G. *Phys. Rev. Lett.* **1999**, *83*, 856.
(44) Chang, E.; Rohlfing, M.; Louie, S. G. *Phys. Rev. Lett.* **2000**, *85*, 2613.
(45) Yamaji, M.; Takehira, K.; Mikoshiba, T.; Tojo, S.; Okada, Y.; Fujitsuka, M.; Majima, T.; Tobita, S.; Nishimura, J. *Chem. Phys. Lett.* **2006**, *425*, 53.
(46) Chaudhuri, D.; Wettach, H.; van Schooten, K. J.; Liu, S.; Sigmund, E.; Höger, S.; Lupton, J. M. *Angew. Chem., Int. Ed.* **2010**, *49*, 7714.
(47) Köhler, A.; Belijonne, D. *Adv. Funct. Mater.* **2004**, *14*, 11.
(48) Barford, W. *Phys. Rev. B* **2004**, *70*, 205204.
(49) Friend, R. H.; Gymer, R. W.; Holmes, A. B.; Burroughes, J. H.; Marks, R. N.; Taliani, C.; Bradley, D. D. C.; Santos, D. A. D.; Brédas, J.-L.; Lögdlung, M.; Salaneck, W. R. *Nature* **1999**, *397*, 121.
(50) Wu, Y.-T.; Hayama, T.; Baldridge, K. K.; Linden, A.; Siegel, J. S. *J. Am. Chem. Soc.* **2006**, *128*, 6870.